

## CRITICAL ROLE OF HELIX 4 OF HIV-1 CAPSID C-TERMINAL DOMAIN IN INTERACTIONS WITH HUMAN LYSYL-tRNA SYNTHETASE

Brandie J. Kovaleski<sup>1</sup>, Robert Kennedy<sup>1</sup>, Ahmad Khorchid<sup>3</sup>, Lawrence Kleiman<sup>3</sup>, Hiroshi Matsuo<sup>2</sup>, and Karin Musier-Forsyth<sup>1,4</sup>†

Departments of <sup>1</sup>Chemistry and <sup>2</sup>Department of Biochemistry, Molecular Biology, and Biophysics, University of Minnesota, Minneapolis, MN 55455; <sup>3</sup>Lady Davis Institute for Medical Research and McGill AIDS Centre, Jewish General Hospital, Montreal, Quebec, Canada H3T 1E2; <sup>4</sup>Departments of Chemistry and Biochemistry, Ohio State University, Columbus, OH 43210

Running head: HIV-1 capsid helix 4 interacts with LysRS

†Address correspondence to: Karin Musier-Forsyth, 100 West 18th Avenue, Columbus, OH 43210.

Office: 614-292-2021. Fax: 614-688-5402. E-mail: [musier@chemistry.ohio-state.edu](mailto:musier@chemistry.ohio-state.edu)

Human tRNA<sup>Lys3</sup> is used as the primer for human immunodeficiency virus type 1 (HIV-1) reverse transcription. HIV-1 Gag and GagPol, as well as host cell factor lysyl-tRNA synthetase (LysRS), are required for specific packaging of tRNA<sup>Lys</sup> into virions. Gag alone is sufficient for packaging of LysRS and these two proteins have been shown to interact *in vitro* with an equilibrium binding constant of ~310 nM. The capsid (CA) domain of Gag binds to LysRS with a similar affinity as full-length Gag. In this work, we report further characterization of the interaction between HIV-1 CA and human LysRS using truncation constructs and point mutations in the putative interaction helices. Fluorescence anisotropy binding measurements reveal that a LysRS variant lacking the N-terminal 219 residues still displays high affinity binding to CA. The CA C-terminal domain (CTD) is also sufficient for binding to LysRS. Nuclear magnetic resonance spectroscopy studies using <sup>15</sup>N-labeled CA-CTD reveal chemical shift perturbations of residues in and proximal to helix 4 of CA-CTD upon LysRS binding. A synthetic peptide that includes helix 4 binds to LysRS with high affinity, whereas peptides derived from the other 3 helical domains of CA-CTD do not. Alanine scanning mutagenesis studies targeting residues in the helix 4 region, support a direct interaction between this domain of CA-CTD and LysRS. The high resolution mapping studies reported here will facilitate future work aimed at disrupting the Gag-LysRS interaction, which represents a novel anti-viral strategy.

Upon infection of a cell by human immunodeficiency virus type 1 (HIV-1)<sup>1</sup>, the viral RNA genome is reverse transcribed into double-stranded proviral DNA. The resulting DNA

translocates into the nucleus and integrates into the host cell's DNA. Transcription of viral DNA yields spliced and unspliced mRNAs, progeny RNA genomes, and viral proteins. Among these viral proteins are two large precursor proteins, Gag and GagPol. During viral maturation, Gag is processed into mature viral proteins matrix, capsid (CA), and nucleocapsid. In the last step of the viral life cycle, Gag, GagPol, genomic RNA, and specific host cell components assemble at the plasma membrane where packaging and assembly of newly formed virus particles occurs.

HIV-1 utilizes human tRNA<sup>Lys3</sup> as the primer for initiating reverse transcription of minus-strand strong-stop DNA (1). The three major tRNA<sup>Lys</sup> isoacceptors, tRNA<sup>Lys1</sup>, tRNA<sup>Lys2</sup>, and tRNA<sup>Lys3</sup>, are selectively packaged into newly forming HIV-1 virions (2). tRNA<sup>Lys1</sup> and tRNA<sup>Lys2</sup> differ from tRNA<sup>Lys3</sup> by 14 and 16 bases, respectively, and from each other by only one base in the anticodon. The fact that all three isoacceptors are packaged, but only tRNA<sup>Lys3</sup> is used as the primer, strongly suggests that lysyl-tRNA synthetase (LysRS) plays a role in specifically targeting tRNA<sup>Lys</sup> for viral packaging. Indeed, human LysRS, the only cellular factor known to interact specifically with all three tRNA<sup>Lys</sup> isoacceptors, is also selectively packaged into HIV-1, independently of tRNA<sup>Lys</sup>, via its interaction with Gag (3). Selective packaging of tRNA<sup>Lys</sup> depends on the synthetase's ability to bind tRNA<sup>Lys</sup>, but aminoacylation activity is not required (4). In addition, the reduction of cytoplasmic LysRS with short interfering RNA results in reduced tRNA<sup>Lys</sup> packaging into virions, reduced tRNA<sup>Lys3</sup> annealing to viral RNA, and reduced viral infectivity (5). Thus, the interaction between host cell LysRS and the HIV-1 packaging machinery,

represents a novel target for the development of anti-HIV therapy.

The minimal complex required for packaging of tRNA<sup>Lys</sup> includes HIV-1 precursor proteins Gag and GagPol, human tRNA<sup>Lys</sup> and LysRS (6). The tRNA<sup>Lys</sup> packaging complex is formed when a Gag/GagPol complex interacts with a tRNA<sup>Lys</sup>/LysRS complex. Gag interacts specifically with LysRS (7) and GagPol interacts with both Gag and tRNA<sup>Lys</sup> (8,9). LysRS can be packaged into viral-like particles composed only of Gag but tRNA<sup>Lys</sup> packaging requires GagPol as well (4). Taken together, these results strongly suggest the importance of the LysRS/Gag interaction in tRNA<sup>Lys</sup> primer packaging.

The regions critical for the protein-protein interaction between LysRS and Gag have been mapped using *in vitro* glutathione *S*-transferase pull-down assays, *in vivo* LysRS viral packaging studies, and studies of Gag-LysRS coimmunoprecipitation from cell lysates (7). The interaction depends on Gag sequences within the C-terminal domain (CTD) of CA and amino acids 208-259 in motif 1 of LysRS. Interestingly, these two regions contain elements involved in the formation of the dimerization interface of each protein. Recent *in vitro* studies show monomer units of each protein interacting to form a heterodimeric Gag/LysRS complex (10).

The crystal structures of *Escherichia coli* LysRS (11) and *Thermus thermophilus* LysRS (12) have been solved. LysRS is a homodimer, with each monomer consisting of an N-terminal anticodon binding domain, a dimerization domain formed by motif 1, and motifs 2 and 3 that together constitute the aminoacylation active site. LysRS is one of the most highly conserved synthetases, and sequence alignments suggest that prokaryotic and eukaryotic LysRSs are structurally similar (13).

Although high resolution structural information for Gag is not available, the crystal structure of the isolated HIV-1 CA-CTD has been solved (14). This domain consists of a 3<sub>10</sub> helix followed by four  $\alpha$ -helices (Figure 1, h1-h4). Dimerization of CA occurs through parallel packing of helix 2 and by packing of the 3<sub>10</sub> helix into a groove created by helices 2 and 3 of the partner molecule.

In this work, we report studies aimed at high resolution mapping of the residues in HIV-1 CA that are involved in interaction with human LysRS. Fluorescence anisotropy (FA) binding

measurements were used to identify minimal constructs of both LysRS and CA-CTD that are still able to interact. Nuclear magnetic resonance (NMR) spectroscopy, alanine scanning mutagenesis, and peptide binding assays are consistent with a critical role for residues in and around the C-terminal helix of CA-CTD.

## EXPERIMENTAL PROCEDURES

**Plasmid Construction**—The plasmids encoding HIV-1 CA (WISP98-85) and HIV-1 CA-CTD (WISP97-07, CA<sub>146-231</sub>) were a gift from Dr. Wesley Sundquist (The University of Utah, Salt Lake City, UT). CA alanine mutants T210A, E212A, M214A, M215A, T216A, H226A, K227A and R229A were constructed using the QuikChange<sup>TM</sup> mutagenesis kit from Stratagene (La Jolla, CA). Residue numbers given throughout this paper refer to CA numbering and not to Gag numbering.

Plasmid pM368 was constructed by cloning a 1.8-Kbp fragment from pM116 into pKS583, a derivative of pET19b (13). The resultant plasmid produces a fusion protein that contains the N-terminal MRGSHHHH-HHHSSGWVD sequence appended to full-length (1–597 amino acids) human LysRS and contains genes conferring ampicillin and chloramphenicol resistance. LysRS  $\Delta$ 1-219 was constructed by amplifying the LysRS gene from residues 220 to 597 while incorporating an Nde1 site near the 5' end and an Xho1 site near the 3' end. In addition, the primer positions an alanine codon on the 5' side of codon 220. The digested PCR product was ligated into Nde1-Xho1 digested pET21b. Candidates were screened by restriction enzyme digestion followed by DNA sequencing.

**Protein Purification and Sample Preparation**—The expression and purification for all CA (10,15) and LysRS (13) proteins was according to previously published procedures. For <sup>15</sup>N CA-CTD labeling, the bacteria were grown in M9 minimal growth medium containing <sup>15</sup>N-ammonium chloride (Cambridge Isotope Laboratories) as the sole nitrogen source. For uniform <sup>13</sup>C/<sup>15</sup>N CA-CTD labeling, the bacteria were grown in M9-medium containing <sup>13</sup>C-glucose (Cambridge Isotope Laboratories) as the sole carbon source and <sup>15</sup>N-ammonium chloride as the sole nitrogen source. Amino acid-specific <sup>15</sup>N-labeled CA-CTD (Leu, Lys, and Val) were

prepared by growing bacteria in M9-medium lacking nitrogen source and supplemented with unlabeled amino acids (100 mg/L each) and the  $^{15}\text{N}$ -labeled amino acid (100 mg/L). The labeled proteins were purified by the same procedure as wild-type proteins.

Samples for NMR experiments contained CA-CTD alone or CA-CTD and LysRS dialyzed into 100 mM ammonium acetate, pH 7, 5 mM tris(2-carboxyethyl)phosphine) and 5%  $\text{D}_2\text{O}$ .

*NMR spectroscopy and data processing*—A 2D  $^1\text{H}$ - $^{15}\text{N}$ -heteronuclear single quantum coherence (HSQC) spectrum of free  $^{15}\text{N}$ -labeled CA-CTD (130  $\mu\text{M}$ ) was collected at 25  $^\circ\text{C}$  on a Varian INOVA 600 MHz spectrometer. The experiment was repeated with the addition of unlabeled human  $\Delta 1$ -219 LysRS (130  $\mu\text{M}$ ). The data were processed and visualized using NMRPipe and NMRdraw, respectively (16).

For peak assignments, NMR spectra were recorded using  $^{15}\text{N}$ ,  $^{13}\text{C}$ -labeled CA-CTD as well as amino acid-specific  $^{15}\text{N}$ -labeled Leu, Lys or Val CA-CTD. Sequential assignment of chemical shift values to backbone atoms was accomplished using conventional triple resonance experiments (17,18).

*Fluorophore Labeling of Protein*—A solution of fluorescein isothiocyanate (FITC) (Invitrogen) was prepared in dimethyl formamide. The concentration of the stock solution of FITC was determined at pH > 9 using the extinction coefficient  $\epsilon_{494\text{nm}} = 73,000 \text{ M}^{-1}\text{cm}^{-1}$ . The CA proteins were labeled with FITC at a 10:1 FITC:protein ratio for 10 min at room temperature in 50 mM HEPES, pH 8. Unreacted dye was removed by buffer exchanging at 4 $^\circ\text{C}$  using a 10,000 MWCO Microcon concentrator (Millipore). Samples were subjected to 10% sodium dodecylsulfate polyacrylamide gel electrophoresis. Ultraviolet illumination of the gels confirmed proteins were labeled and contained little or no free fluorophore.

*Solid Phase Peptide Synthesis of CA-CTD-Derived Helices*—Helix h1 (158-174: KEPFRDYVDRFYKTLRA) and h3 (194-204: ANPDKTILKA) of HIV-1 CA-CTD were synthesized by standard solid-phase methods. Labeling at the N-terminal amine of each peptide was achieved by addition of a 10-fold molar excess of FITC in DMF (pH  $\sim$  9) while the peptide

was still resin-bound (at the C-terminus) and each amino acid was still side-chain protected. Following an overnight incubation, peptides were cleaved from the resin, purified by reversed phase high performance liquid chromatography, and confirmed by mass spectrometry.

Helix h2 (176-190: QASQEVKNWMTETLL) and h4 (211-227: LEEMMTACQVGGPGHK) of HIV-1 CA-CTD were obtained through the AIDS Research and Reference Reagent Program. Peptides were received in purified, lyophilized form and reconstituted in water. Labeling with FITC was achieved essentially as described above. FITC reacts with non-protonated aliphatic amine groups, including the amine terminus of proteins or peptides and the amino group of lysines. Thus, labeling of h2/h4 peptides results in the possibility of the label being attached at either the N-terminus or at lysine residues within the peptides (K182 of h2 or K227 of h4). Selective labeling of the N-terminus is favored at pH 7 and thus, these reactions were performed at lower pH. High performance liquid chromatography purification followed by mass spectrometry analysis confirmed a 1:1 peptide:dye ratio.

*Circular Dichroism (CD) Analysis*—CD spectra of wild-type and truncated LysRS and CA were measured at room temperature using a J-710 spectropolarimeter (Jasco) with a 0.1 mm path-length cuvette. Prior to analysis, proteins were dialyzed into 10 mM  $\text{NaPO}_4$ , pH 7.5, and diluted to a concentration of 5  $\mu\text{M}$ . Spectra were accumulated over six scans.

CD spectra of each synthesized peptide was also recorded and used to confirm the helical nature of each. Peptides were dissolved in water to a final concentration of 1 mg/ml and 2,2,2-trifluoroethanol (TFE) was added to 25% (19).

*Fluorescence Anisotropy (FA) Measurements*—Equilibrium dissociation constants were determined by measuring the FA of 50 nM fluorescently-labeled species (CA:FITC, CA-CTD:FITC or peptide:FITC) as a function of increasing concentrations of unlabeled protein (LysRS or  $\Delta 1$ -219 LysRS). The labeled protein was incubated with varying amounts of the desired unlabeled protein for 30 min at room temperature in 20 mM HEPES, pH 7.5, and 50 mM NaCl. Anisotropy measurements were made either on a Photon Technology International spectrofluorimeter (Model QM-2000) or on an

Analyst AD fluorescence plate reader (Molecular Devices). The excitation and emission wavelengths were 490 nm and 520 nm, respectively (slit widths = 5 nm). Data analysis was performed as previously described (10).

*Docking Model of LysRS and CA*—A homology model of human LysRS was generated using the program MODELLER 4 (20). The available coordinates from the X-ray structure of *E. coli* LysRS (1E1O) were used as a template (11).

LysRS-CA docking studies were performed using the Chimera/BiGGER software package. The docking models of LysRS-CA were generated using the algorithms implemented in Chimera 2.0 (21). BiGGER was run with two docking partners, selecting the monomeric CA structure (Protein Data Bank code 1E6J chain P) as the probe, and the modeled structure of human LysRS as the target. The first round of docking experiments factored in the protein geometry, electrostatic contacts, as well as hydrophobic interactions. The parameters used were as follows: resolution 1.0; added radius of 1.0; angular steps of 15 with a minimal overlap of 100. Ten thousand solutions were obtained by this procedure. After the docking run, models were filtered using a 4 Å cutoff to give 2000 unique clusters. The docking models were scored based on the *in vivo* data generated from deletion mapping of the binding regions of LysRS and Gag (7).

## RESULTS

*FA Binding Assays Show Interaction Between Minimal Gag and LysRS Constructs*—Previous studies mapped the regions critical for the LysRS/Gag interaction to Gag sequences within CA-CTD and amino acids within motif 1 of LysRS (7). *In vitro* binding assays also revealed that CA binds LysRS with a similar affinity as full-length Gag (~420 nM) (10). To further delineate the minimal domains required for the LysRS/Gag interaction, we prepared two truncation mutants. The CTD of CA has previously been purified and shown to fold independently of the N-terminal domain (22). The CA-CTD construct encoding residues 146 to 231 of CA was purified from *E. coli*. Expression and purification of a truncation mutant of human LysRS lacking 219 residues from the N-terminus ( $\Delta$ 1-219 LysRS) was also carried out. This LysRS construct preserves the catalytic domain of LysRS

but lacks the anticodon binding domain and the N-terminal extension. CD analysis indicated that  $\Delta$ 1-219 LysRS appeared to be folded in a similar manner to wild-type LysRS (data not shown). FA measurements showed that the binding affinity between  $\Delta$ 1-219 LysRS and CA-CTD was only ~2-fold reduced relative to the full-length proteins ( $K_d = 770 \pm 160$  nM, Figure 2). These *in vitro* experiments validate an earlier *in vivo* observation that  $\Delta$ 1-207 LysRS is incorporated into Gag VLPs approximately 70% as efficient as WT LysRS, and supports previous data mapping the LysRS/Gag interaction to the CTD of CA and the catalytic domain of LysRS (7).

*NMR Studies of Minimal Gag and LysRS Constructs*—The sequential assignment of NMR signals of  $^1\text{H}^{15}\text{N}$ ,  $^{15}\text{N}$ ,  $^{13}\text{C}\alpha$  and  $^{13}\text{C}\beta$  atoms of CA-CTD was achieved, with the exception of amino acids 147-153 and 172-192. These residues are located at the monomer-dimer interface, and due to the relatively weak dimer (full-length CA  $K_d = 18 \pm 1$   $\mu\text{M}$ ; CA-CTD  $K_d = 10 \pm 3$   $\mu\text{M}$ ) and a heterogeneous dimer interface (22), their amide nitrogen and amide proton correlation signals were broadened and missing from the spectra.

Chemical shift perturbation of  $^{15}\text{N}$ -labeled-CA-CTD was observed upon addition of unlabeled  $\Delta$ 1-219 LysRS. A 2D  $^1\text{H}$ - $^{15}\text{N}$ -heteronuclear single quantum coherence (HSQC) spectrum of free  $^{15}\text{N}$ -labeled CA-CTD is shown in Figure 3A (black peaks). In this spectrum, main chain amide protons are observed, with one signal for each residue. The same experiment was also performed in the presence of equimolar amounts of unlabeled  $\Delta$ 1-219 LysRS (Figure 3A, red peaks). While many peaks did not change upon LysRS addition, 9 peaks displayed small to moderate chemical shift perturbations (Figure 3A). Interestingly, all the shifted residues are either in or proximal to helix 4 of CA-CTD. The largest perturbations occur at positions T210 and H226, which are located at the N-terminus of helix 4 and in the adjacent C-terminal tail, respectively (Figure 3B).

*FA Binding Studies Between CA-CTD-Derived Peptides and LysRS*—To further probe the interaction between CA-CTD and LysRS, four peptides derived from h1-h4 of the CA-CTD were labeled with FITC (Figure 1). The helical nature of each peptide was verified by CD spectroscopy measurements performed in 25% TFE (data not shown). All four CA-derived helices were tested

for their ability to bind LysRS using FA measurements. The peptides were kept at a constant concentration of 50 nM and LysRS was varied from 0-20  $\mu$ M. Strikingly, the peptide derived from h4 was the only peptide that showed significant binding to LysRS ( $K_d = 270 \pm 60$  nM; Figure 4). Little or no binding of peptides derived from h1, h2, or h3 was observed (Figure 4; inset). These data support the NMR findings and suggests that h4 plays a critical role in CA-CTD binding to LysRS.

*Alanine-Scanning Mutagenesis*—Based on the NMR results shown in Figure 3 and the helix binding data shown in Figure 4, eight point mutants in the predicted h4 interacting region of CA-CTD were prepared. FA was used to test the effect of each single point mutant on CA-CTD binding to LysRS. As shown in Table 1, mutations to alanine at positions T210, M214, M215, and H226 have significant (~3-fold) effects on the binding affinity. An alanine substitution at E212 had a more modest 2-fold effect. Changes at T216, K227, and R229 had little or no effect on binding to LysRS. Taken together, these results support the NMR and peptide binding studies, suggesting a critical role for h4 in binding to LysRS.

*Docking Model of Human LysRS and HIV-1 CA*—Figure 5 shows a model generated from LysRS-CA docking studies. In these studies, multiple high scoring models were clustered into three basic binding modes. One of these three modes, shown in Figure 5, correlates well with the NMR data, FA peptide binding studies, and alanine scanning mutagenesis, and shows a close interaction of CA-CTD h4 to the polar face of the amphoteric helix H7 of LysRS.

## DISCUSSION

Disruption of the Gag-LysRS interaction, which is essential for specific tRNA<sup>Lys</sup> primer packaging, represents a novel therapeutic strategy. As a first step toward this goal, we have begun to map the interaction domain at high resolution. In this work, minimal constructs of HIV-1 Gag (CA-CTD) and human LysRS ( $\Delta$ 1-219 LysRS) have been identified and used in NMR chemical shift perturbation experiments. These studies show that residues within and flanking helix 4 of CA-CTD are perturbed upon LysRS binding. Based on the crystal structure of the isolated HIV-1 CA-CTD, dimerization of CA can occur through parallel

packing of helix 2 (14). Interestingly, a recent X-ray structure of CA-CTD containing a single alanine deletion (residue 177) revealed a significantly different dimer interface (23). The mutant structure is described as a domain-swapped homolog of the wild-type protein, with the dimer formed by exchange of the protein segment that contains the N-terminal strand and helix 1 between the two monomers. In this structure, the major homology region (MHR) in helix 1, a highly conserved domain present in all retroviral CA proteins (24), forms a major part of the dimer interface, providing an explanation for the conservation of the MHR, as well as its critical role in assembly (25,26). Importantly, helix 4 is not intimately involved in the dimer interface of either structure, and is therefore available for interaction with other proteins, such as LysRS.

In all three wild-type crystal structures of the CA-CTD (14,22) there is a disulfide bond between Cys198 and Cys218 that links the N-terminus of helix 3 to the C-terminus of helix 4. In freshly lysed viral particles, Cys218 is present as a free thiol (14). It has been proposed that disulfide bond formation may modulate CA-CA interactions and facilitate uncoating of the core structure upon infection. With the exception of this possible disulfide bond, helix 4 has not, to our knowledge, been reported to be involved in any protein-protein interactions.

The observed chemical shift perturbations were consistent with an interaction between LysRS and residues in and proximal to helix 4 of CA-CTD. This conclusion is strongly supported by peptide binding studies (Figure 4) and alanine scanning mutagenesis data (Table 1). The largest NMR perturbations occurred at positions T210 and H226. The latter residue also displayed significantly reduced peak intensity upon LysRS addition. This result is consistent with a direct interaction, and indeed individually mutating these two residues to alanine resulted in a significant (~3-fold) decrease in binding affinity to LysRS. Although K227 and R229 undergo modest chemical shift changes, mutation of these residues does not result in altered binding affinity, suggesting that they do not directly interact with LysRS. The direct interaction of nearby residues such as H226, may have induced a structural change that resulted in the observed chemical shift changes. Surprisingly, mutations at M214 and

M215, residues that did not shift in the NMR experiments, also resulted in similar decreases in binding affinity. Helix 4 is only 6 amino acids long and M214/M215 are in the middle of the helix. Mutation of these residues may have resulted in a conformational change that affected the binding of LysRS although they are not directly involved in the interaction.

In summary, we have localized the LysRS interaction domain on Gag to the residues within and proximal to h4 of the CA-CTD. Previous

LysRS mapping studies, together with computational docking studies carried out here (Figure 5), support a direct interaction between h4 of CA-CTD and H7 of LysRS. High resolution mapping of the interaction surface on H7 is underway. Taken together, these results will help to inform both rational design and screening approaches to find inhibitors of this novel anti-HIV target.

*Acknowledgements*—We greatly appreciate the gift of plasmids encoding HIV-1 CA and CA-CTD from Wesley I. Sundquist (The University of Utah, Salt Lake City, UT). We thank Dr. Daniel Mullen for his assistance in the synthesis and purification of peptides. This work was supported by N.I.H. Grant AI054145 (to L.K. and K.M.-F.), Ruth L. Kirschstein National Service Award GM069339 (R.K.) and T32-GM08700 (B.J.K.).

## REFERENCES

1. Jiang, M., Mak, J., Ladha, A., Cohen, E., Klein, M., Rovinski, B., and Kleiman, L. (1993) *J Virol* **67**, 3246-3253
2. Mak, J., and Kleiman, L. (1997) *J Virol* **71**, 8087-8095
3. Cen, S., Khorchid, A., Javanbakht, H., Gabor, J., Stello, T., Shiba, K., Musier-Forsyth, K., and Kleiman, L. (2001) *J Virol* **75**, 5043-5048
4. Cen, S., Javanbakht, H., Niu, M., and Kleiman, L. (2004) *J Virol* **78**, 1595-1601
5. Guo, F., Cen, S., Niu, M., Javanbakht, H., and Kleiman, L. (2003) *J Virol* **77**, 9817-9822
6. Kleiman, L., and Cen, S. (2004) *Int J Biochem Cell Biol* **36**, 1776-1786
7. Javanbakht, H., Halwani, R., Cen, S., Saadatmand, J., Musier-Forsyth, K., Gottlinger, H., and Kleiman, L. (2003) *J Biol Chem* **278**, 27644-27651
8. Park, J., and Morrow, C. D. (1992) *J Virol* **66**, 6304-6313
9. Mak, J., Jiang, M., Wainberg, M. A., Hammarskjold, M. L., Rekosh, D., and Kleiman, L. (1994) *J Virol* **68**, 2065-2072
10. Kovaleski, B. J., Kennedy, R., Hong, M. K., Datta, S. A., Kleiman, L., Rein, A., and Musier-Forsyth, K. (2006) *J Biol Chem* **281**, 19449-19456
11. Onesti, S., Miller, A. D., and Brick, P. (1995) *Structure* **3**, 163-176
12. Cusack, S., Yaremchuk, A., and Tukalo, M. (1996) *EMBO J* **15**, 6321-6334
13. Shiba, K., Stello, T., Motegi, H., Noda, T., Musier-Forsyth, K., and Schimmel, P. (1997) *J Biol Chem* **272**, 22809-22816
14. Worthylake, D. K., Wang, H., Yoo, S., Sundquist, W. I., and Hill, C. P. (1999) *Acta Crystallogr D Biol Crystallogr* **55**, 85-92
15. Yoo, S., Myszka, D. G., Yeh, C., McMurray, M., Hill, C. P., and Sundquist, W. I. (1997) *J Mol Biol* **269**, 780-795
16. Delaglio, F., Grzesiek, S., Vuister, G. W., Zhu, G., Pfeifer, J., and Bax, A. (1995) *J Biomol NMR* **6**, 277-293
17. Matsuo, H., Kupce, E., Li, H., and Wagner, G. (1996) *J Magn Reson B* **111**, 194-198
18. Powers, R., Garrett, D. S., March, C. J., Frieden, E. A., Gronenborn, A. M., and Clore, G. M. (1992) *Biochemistry* **31**, 4334-4346
19. Listowsky, M. G. a. I. (1962) *J Am Chem Soc* **84**, 3770 - 3771
20. Sali, A. (1995) *Mol Med Today* **1**, 270-277
21. Palma, P. N., Krippahl, L., Wampler, J. E., and Moura, J. J. (2000) *Proteins* **39**, 372-384

22. Gamble, T. R., Yoo, S., Vajdos, F. F., von Schwedler, U. K., Worthylake, D. K., Wang, H., McCutcheon, J. P., Sundquist, W. I., and Hill, C. P. (1997) *Science* **278**, 849-853
23. Ivanov, D., Tsodikov, O. V., Kasanov, J., Ellenberger, T., Wagner, G., and Collins, T. (2007) *Proc Natl Acad Sci U S A* **104**, 4353-4358
24. Wills, J. W., and Craven, R. C. (1991) *AIDS* **5**, 639-654
25. Strambio-de-Castillia, C., and Hunter, E. (1992) *J Virol* **66**, 7021-7032
26. Mammano, F., Ohagen, A., Hoglund, S., and Gottlinger, H. G. (1994) *J Virol* **68**, 4927-4936

## FOOTNOTE

<sup>1</sup>The abbreviations used are: HIV-1, human immunodeficiency virus type 1; LysRS, lysyl-tRNA synthetase; FA, fluorescence anisotropy; CTD, C-terminal domain; CA, capsid protein; FITC, fluorescein isothiocyanate; CD, circular dichroism; TFE, trifluoroethanol; NMR, nuclear magnetic resonance; HSQC, heteronuclear single quantum coherence.

## FIGURE LEGENDS

FIG. 1. **HIV-1 CA-CTD sequence and secondary structure.** Helices are color-coded as follows: 3<sub>10</sub> helix (residues 149-152), blue;  $\alpha$ -helix 1 (h1, residues 161-174), red;  $\alpha$ -helix 2 (h2, residues 179-192), purple;  $\alpha$ -helix 3 (h3, residues 196-205), cyan;  $\alpha$ -helix 4 (h4, residues 211-217), green (14). The four synthetic peptides derived from h1-h4 are indicated by the solid bars and numbering below each helix.

FIG. 2. **FA binding analysis of minimal constructs  $\Delta$ 1-219 LysRS and CA-CTD.** The binding affinity of  $\Delta$ 1-219 LysRS to CA-CTD:FITC was determined by measuring FA of 50 nM CA-CTD:FITC as a function of increasing concentrations of  $\Delta$ 1-219 LysRS. A representative data set is shown, but the measurement was carried out three times with the standard deviation indicated.

FIG. 3. **NMR analysis of HIV-1 CA-CTD.** (A) HSQC spectra of <sup>15</sup>N-labeled CA-CTD alone (black) and in the presence of an equimolar ratio of  $\Delta$ 1-219 LysRS (red). Peaks that undergo chemical shift perturbations upon LysRS addition are labeled. (B) A close up view of the most significant chemical shift changes.

FIG. 4. **FA binding analysis of individual CA-CTD helices and LysRS.** Binding of the four peptides shown in Figure 1 to LysRS was measured using 50 nM fluorescently labeled peptides as a function of increasing concentrations of LysRS. Helix 4 is the only peptide that demonstrated significant binding affinity (main graph) while h1-h3 displayed weak or no binding (inset).

FIG. 5. **Docking Model of CA-CTD and LysRS.** Predicted mode of LysRS-CA interaction based on computational docking studies carried out as described in the experimental procedures. LysRS helices and beta sheets outside of the putative interacting domains are colored in cyan and magenta, respectively. The putative CA (Gag) binding region is in gold and these helices are marked by an upper case H. The CA-CTD helices are indicated by a lower case h with h1 in red, h2 in orange, h3 in blue and h4 in green.

**TABLE 1**

Apparent equilibrium dissociation constants ( $K_d$ ) for human LysRS binding to wild-type (WT) and mutant FITC-labeled CA variants obtained from fluorescence anisotropy measurements<sup>a</sup>

Interacting Protein	$K_d$ (nM)
CA (WT)	420 ± 10
T210A	1520 ± 330
E212A	870 ± 190
M214A	1300 ± 390
M215A	1470 ± 80
T216A	660 ± 40
H226A	1160 ± 320
K227A	305 ± 220
R229A	500 ± 220

<sup>a</sup>Measurements were performed in the presence of 40 mM HEPES, pH 7.5, and 50 mM NaCl. Results are the average of 3 trials with the standard deviation indicated.

Figure 1

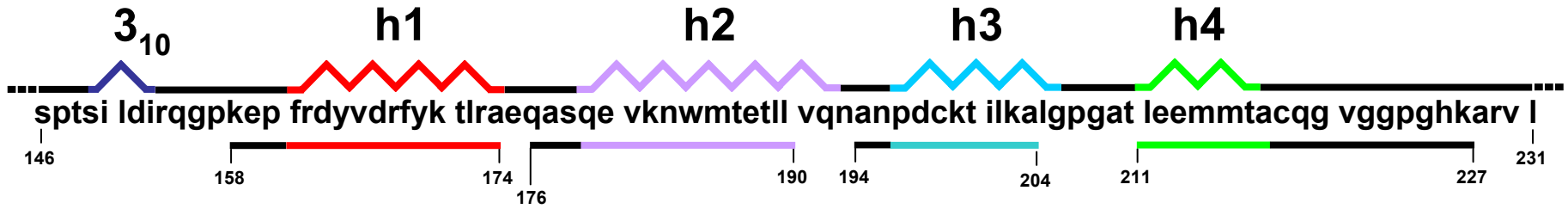


# Figure 2

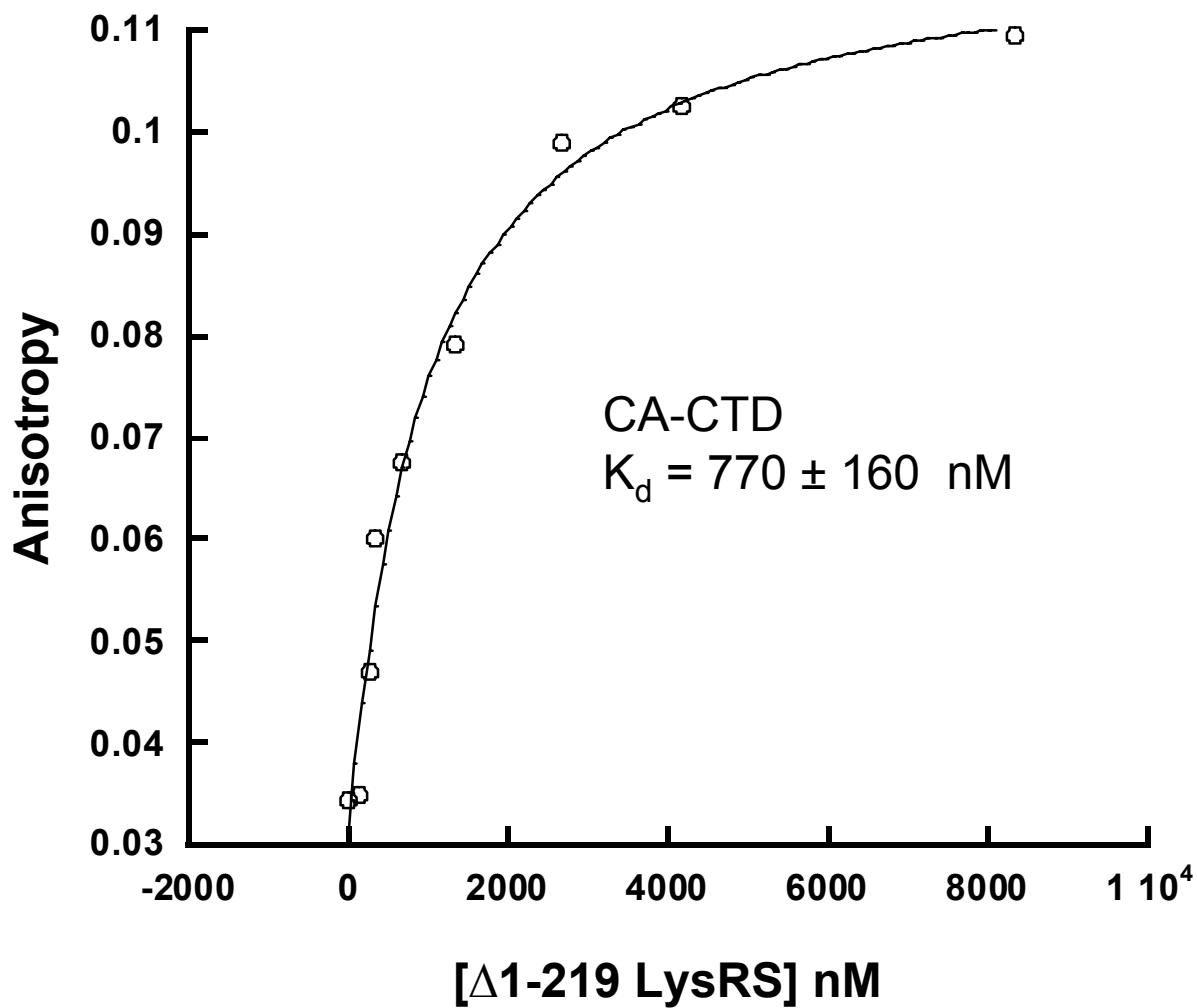


# Figure 3

## A

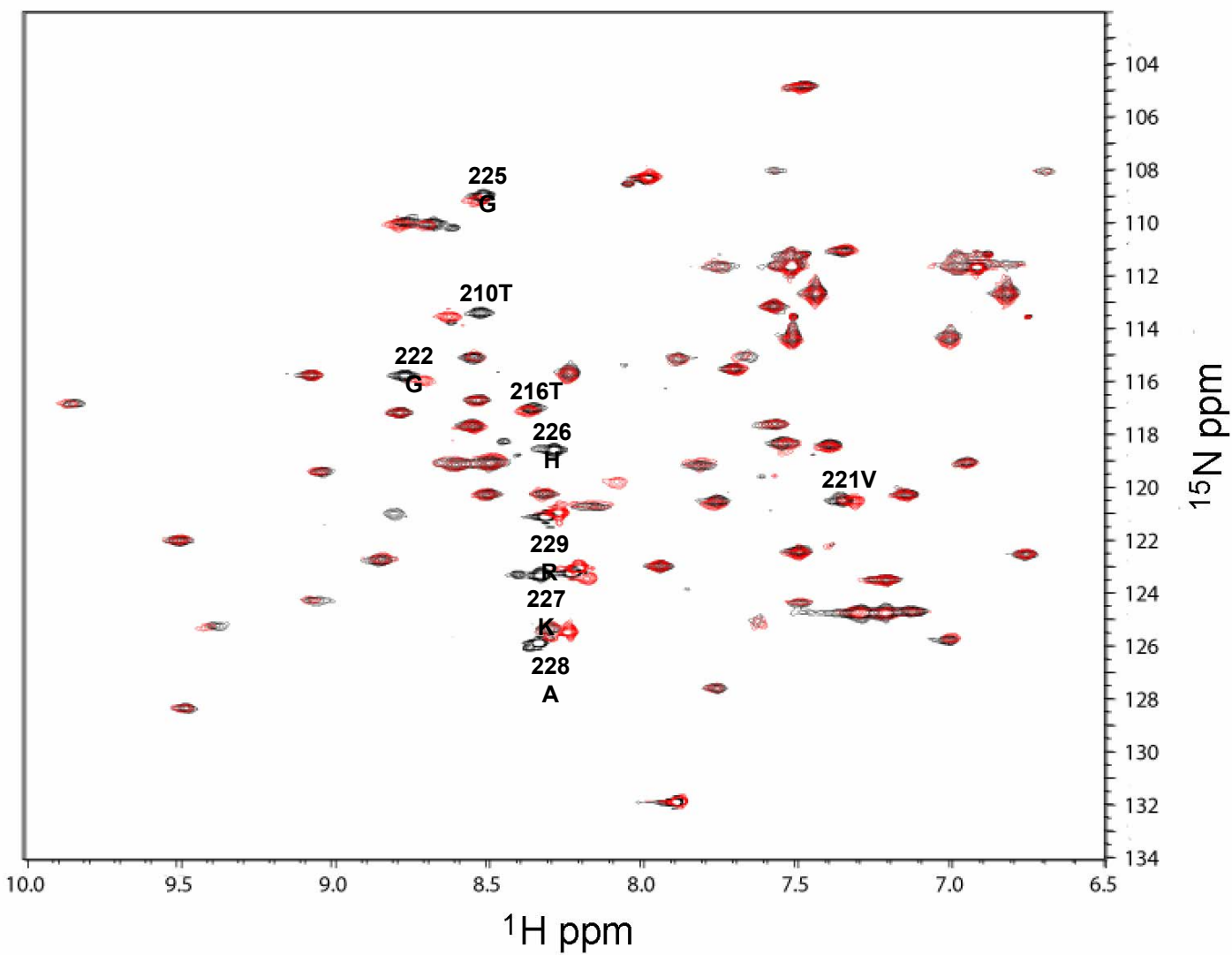
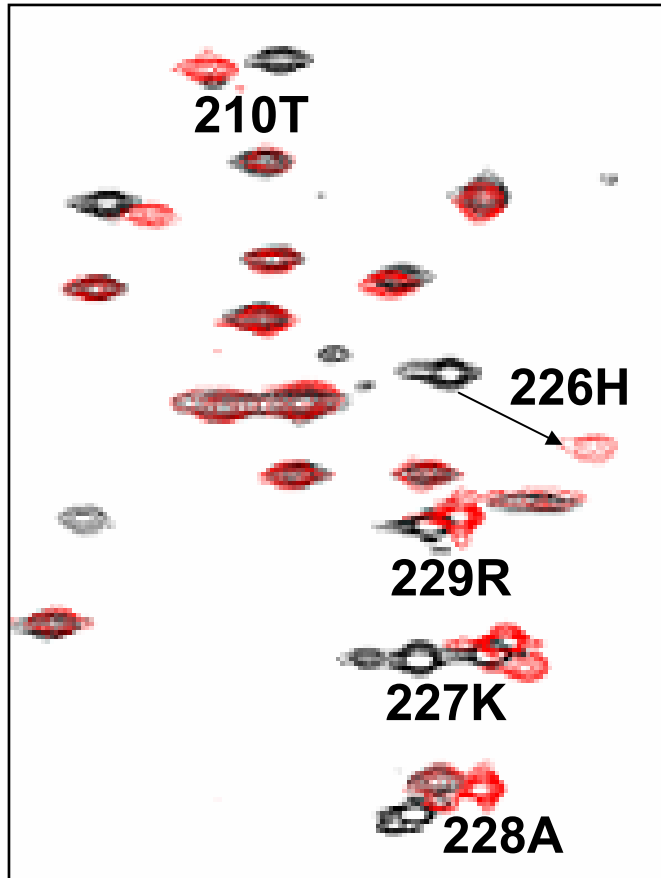


Figure 3

**B**



# Figure 4

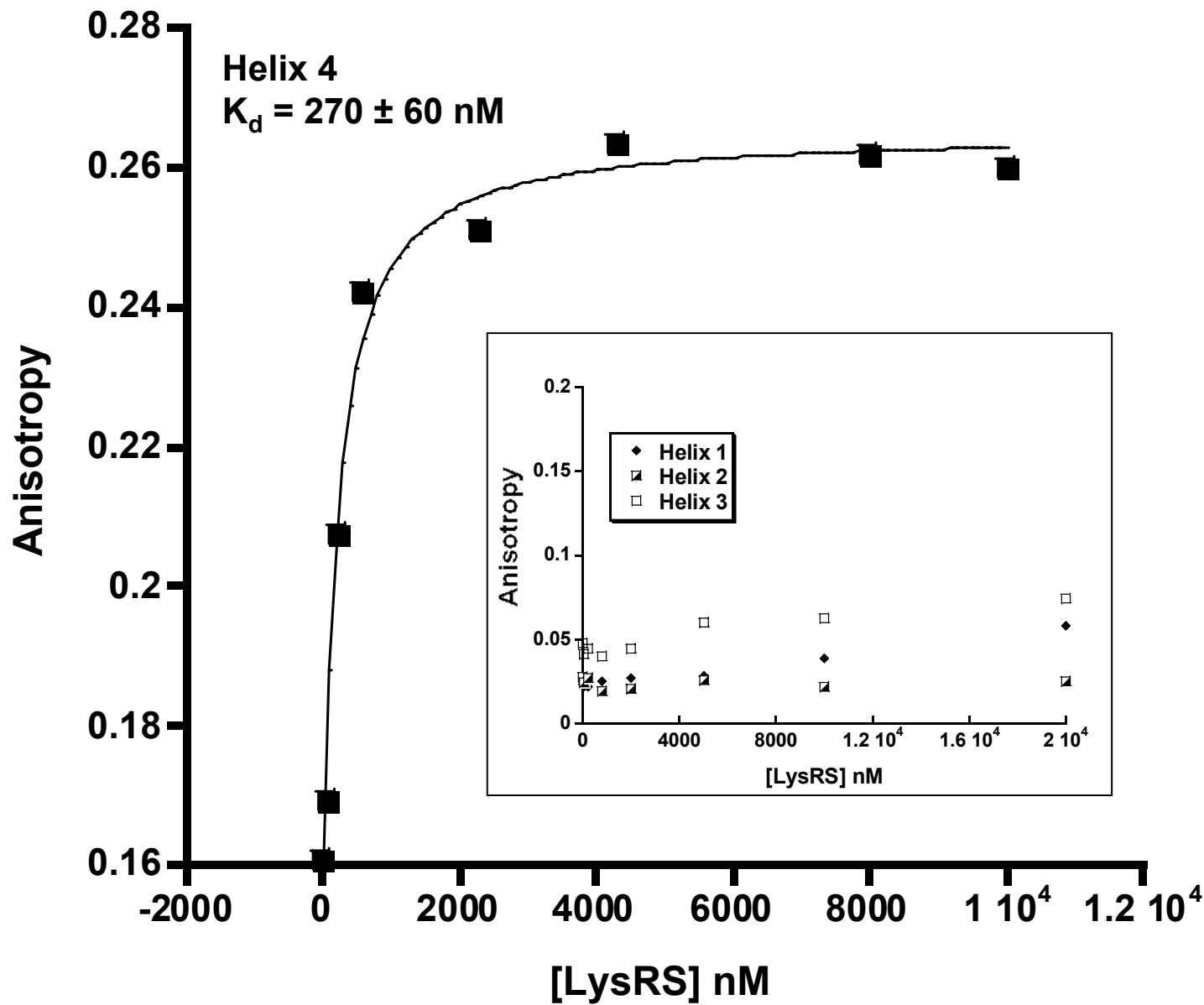


Figure 5

